Lithium Insertion in Copper, Indium, Tin Thiospinels Characterized by ^{119}Sn Mössbauer Spectroscopy and Rietveld Analysis

R. Dedryvère,* J. Olivier-Fourcade, and J. C. Jumas

Laboratoire des Agrégats Moléculaires et Matériaux Inorganiques (UMR 5072), Université Montpellier II, CC15, place Eugène Bataillon, 34095 Montpellier, France

S. Denis

Laboratoire de Réactivité et Chimie des Solides (UPRES-A 6007) 33, rue Saint-Leu, 80039 Amiens Cedex, France

C. Pérez Vicente

Laboratorio de Química Inorgánica, Facultad de Ciencias, Universidad de Córdoba, Avda. San Alberto Magno s/n, 14004 Córdoba, Spain

Received December 8, 1999

Chemical lithium insertion via *n*-butyllithium was carried out on a family of spinel phases of the $Cu_2S-In_2S_3-SnS_2$ system, of general formula $Cu_{0.5+\alpha}In_{2.5-3\alpha}Sn_{2\alpha}S_4$, $0 \le \alpha \le 0.5$. Structural analyses were performed by X-ray and neutron powder diffraction (Rietveld method) and ^{119}Sn Mössbauer spectroscopy. Two mechanisms of lithium insertion occur at the same time. The first is characterized by the reduction of Sn^{IV} into Sn^{II} and a spinel to rocksalt transformation. The second leads to the total reduction of tin cations into Sn^0 and the formation of metallic bonds in an amorphous phase. The relative amounts of indium and tin are discussed with respect to the crystallinity of the rocksalt phase. An electrochemical study was carried out to evaluate the cycling behavior of these compounds, and their possible use as anode material in lithium ion cells.

Introduction

Compounds with spinel-related structure provide suitable host materials for insertion of lithium ions. The presence of a great number of empty sites is particularly favorable for incorporation of guest ions and allows a three-dimensional insertion. These properties make materials with spinel-related structures interesting candidates for applications as electrodes in lithium ion batteries.[1−3]

The general formula of spinel compounds can be represented as AB_2X_4. The space group is $Fd\bar{3}m$. The unit cell contains 32 X anions on the 32e sites (cubic close-packing arrangement), 8 A cations on 8a sites (tetrahedrally coordinated by anions), and 16 B cations on 16d sites (octahedrally coordinated). Nevertheless, A cations can also occupy 16d sites and some B cations 8a sites, to give an inverse spinel. It is also possible to find cation-deficient spinels, thus increasing the number of available sites for intercalation.

Post-transition metals of groups 13 and 14 provide many examples of sulfide compounds having a spinel-related structure. Particularly, ternary indium and tin thiospinel compounds such as $M_{0.5}In_{2.5}S_4$ (M = Cu, Ag), MIn_2S_4 (M = Mn, Fe, Co, Ni), $CuM_{0.5}Sn_{1.5}S_4$ (M = Mn, Fe, Co, Ni), and the cation-deficient $In_2Sn_{0.5}S_4$ have been previously studied as host lattices for lithium insertion by both chemical and electrochemical methods.[4−7]

In the present work, we have carried out the structural characterization of pristine and chemically lithiated products for a series of compounds of general formula $Cu_{0.5+\alpha}In_{2.5-3\alpha}Sn_{2\alpha}S_4$ ($0 \le \alpha \le 0.5$). This family of compounds is placed in the domain of spinel-related structure of the pseudoternary phase diagram $Cu_2S-In_2S_3-SnS_2$.[8] Different compounds with α varying from 0 ($Cu_{0.5}In_{2.5}S_4$) to 0.5 ($CuInSnS_4$) have been characterized before and after chemical lithium insertion (via *n*-butyllithium) by X-ray and neutron powder diffraction (Rietveld method) and ^{119}Sn Mössbauer spectroscopy, to establish the mechanism of lithiation. Electrochemical lithium insertion was also carried out to evaluate the cycling behavior of these materials for possible application as negative electrode in lithium ion batteries.

* Corresponding author. E-mail: rdedry@crit.univ-montp2.fr

(1) Eisenberg, M. *J. Electrochem. Soc.* **1980**, *127*, 2382.
(2) Thackeray, M. M.; David, W. I. F.; Goodenough, J. B. *Mater. Res. Bull.* **1982**, *17*, 785.
(3) James, A. C. W. P.; Ellis, B.; Goodenough, J. B. *Solid State Ionics* **1988**, *27*, 45.
(4) Bousquet, C.; Krämer, A.; Pérez Vicente, C.; Tirado, J. L.; Olivier-Fourcade, J.; Jumas, J. C. *J. Solid State Chem.* **1997**, *134*, 238.
(5) Morales, J.; Tirado, J. L.; Elidrissi-Moubtassim, M. L.; Olivier-Fourcade, J.; Jumas, J. C. *J. Alloys Compd.* **1995**, *217*, 176.
(6) Elidrissi-Moubtassim, M. L.; Olivier-Fourcade, J.; Jumas, J. C.; Senegas, J. *J. Solid State Chem.* **1990**, *87*, 1.
(7) Lavela, P.; Tirado, J. L.; Morales, J.; Olivier-Fourcade, J.; Jumas, J. C. *J. Mater. Chem.* **1996**, *6* (1), 41.
(8) Ohachi, T.; Pamplin, B. R. *J. Crystal Growth* **1977**, *42*, 598.

10.1021/cm991190j CCC: $19.00
Published on Web 04/21/2000

Experimental Section

All compounds were synthesized by solid-state reaction. Stoichiometric amounts of the binary sulfides Cu_2S, In_2S_3, and SnS_2 were mixed and sealed in silica tubes under vacuum at $\sim 10^{-3}$ Pa. The mixture was slowly heated at 1 °C/min to 400 °C and held for 10 h, then to 750 °C for 10 h, and finally to 850 °C for 5 days. The samples were then slowly cooled to room temperature. Six different compounds were prepared: $Cu_{0.5}In_{2.5}S_4$, $Cu_{0.6}In_{2.2}Sn_{0.2}S_4$, $Cu_{0.65}In_{2.05}Sn_{0.3}S_4$, $Cu_{0.73}In_{1.82}Sn_{0.45}S_4$, $Cu_{0.75}In_{1.75}Sn_{0.5}S_4$, and $CuInSnS_4$, corresponding to $\alpha = 0$, 0.1, 0.15, 0.23, 0.25, and 0.5 respectively in $Cu_{0.5+\alpha}In_{2.5-3\alpha}Sn_{2\alpha}S_4$.

Chemical lithium insertion was carried out using the *n*-butyllithium technique.[2,6] The powder samples were suspended 24 h in solutions of (n-C_4H_9)Li in hexane with increasing concentrations (up to 0.37 mol/L). A thermostatic bath was used to keep the temperature constant at 35 °C and the experimental device was kept under a dry argon atmosphere during the reaction. The treated samples were collected, filtered, washed with dry hexane and stored in an argon-filled glovebox to avoid side oxidation reactions. The determination of the amount of inserted lithium was performed by atomic emission spectroscopy using a Jobin Yvon JY24 spectrophotometer (Inductively Coupled Plasma).

Electrochemical lithiation was carried out with Li/$LiPF_6$ 1 M (EC:DMC)/sulfospinel Swagelock test cells as described elsewhere.[9] Galvanostatic charge/discharge curves were obtained with a cycling rate of 1 Li/4 h for the first cycle, and 1 Li/2 h for tests of capacity loss (range 0−2.5 V).

X-ray powder diffraction (XRD) characterization was performed by a Philips $\theta - 2\theta$ diffractometer using Cu Kα radiation and a nickel filter. Neutron diffraction patterns were recorded on the D1B apparatus at the Laue−Langevin Institute (Grenoble, France) at the wavelength 1.28 Å, at room tempetrature. To analyze structural modifications induced by lithium insertion, Rietveld analyses of XRD patterns were carried out with the aid of the program "Rietveld Analysis Program DBWS-9411".[10]

Pristine and lithiated samples were studied by ^{119}Sn Mössbauer spectroscopy using a conventional EG&G constant-acceleration spectrometer. The γ-ray source was ^{119m}Sn in a $BaSnO_3$ matrix, working at room temperature. Recorded spectra were fitted with Lorentzian profiles by the least-squares method using the program ISO,[11] and the fit quality was controlled by the χ^2 test. All isomer shifts are given relative to ^{119}Sn in $BaSnO_3$.

Results and Discussions

A. Pristine $Cu_{0.5+\alpha}In_{2.5-3\alpha}Sn_{2\alpha}S_4$ Samples. The XRD patterns of all pristine compounds were characteristic of single-phase products and could be indexed in the cubic system. Rietveld analyses confirmed the spinel structure with the $Fd\bar{3}m$ space group,[12] according to the following cation distribution and formal oxidation states: $(Cu^{I}_{4+8\alpha}In^{III}_{4-8\alpha})_{8a}\,[In^{III}_{16-16\alpha}Sn^{IV}_{16\alpha}]_{16d}\,\{S_{32}\}_{32e}$.

As previously reported, the crystal structure of $Cu_{0.5}In_{2.5}S_4$ ($\alpha = 0$) is described in the $F\bar{4}3m$ space group,[13−15] due to a partial ordering of copper atoms and resulting in a split of the 8a sites in two sets of positions (4a and 4b in $F\bar{4}3m$), and thus decreasing the symmetry of the solid. Nevertheless, when the samples are prepared as powders, a better fit is obtained with the $Fd\bar{3}m$ space group, as reported by Colombet et al.[16] Table 1 includes the fitted structural parameters and the reliability factors. The evolution of the unit cell parameter a in the solid solution $Cu_{0.5+\alpha}In_{2.5-3\alpha}Sn_{2\alpha}S_4$ ($0 \le \alpha \le 0.5$) as a function of α is linear, according to Vegard's law. The value obtained for $\alpha = 0.5$ is in good agreement with previously reported data.[16,17]

Table 1. Results of the Rietveld Analysis of Spinel Phases of the Solid Solution $Cu_{0.5+\alpha}In_{2.5-3\alpha}Sn_{2\alpha}S_4$, $0 \le \alpha \le 0.5$, with $Fd\bar{3}m$ Space Group, Origin Choice 2 ($\bar{3}m$)[a]

sample	$\alpha = 0$	$\alpha = 0.1$	$\alpha = 0.23$	$\alpha = 0.25$	$\alpha = 0.5$
			Cell Parameters		
a (Å)	10.688(1)	10.655(1)	10.595(1)	10.587(1)	10.488(1)
$x_{(32e)}$	0.255(1)	0.255(1)	0.254(1)	0.255(1)	0.254(1)
			Reliability Factors		
R_{Bragg}	4.23	2.73	2.92	2.95	1.94
R_p	7.20	6.02	4.28	8.47	4.28
R_{wp}	9.21	7.74	5.54	10.60	5.83
$R_{expected}$	7.40	6.18	5.09	5.43	5.48
GoF	1.24	1.25	1.08	1.93	1.06

[a] Atoms have been placed in the following sites: 8a ($4 + 8\alpha$ Cu and $4 - 8\alpha$ In), 16d ($16 - 16\alpha$ In $+ 16\alpha$ Sn) and 32e (32 S). Alpha was not refined but was given the nominal value.

^{119}Sn Mössbauer spectra were characterized by the presence of only one unresolved split signal. The isomer shifts of $\sim$1.12−1.14 mm s^{-1} are in the range of the typical values observed for Sn^{IV} in sulfides and the quadrupole splitting of $\sim$0.2−0.3 mm s^{-1} is characteristic of a slightly distorted octahedral coordination. It confirms the cation distribution proposed above.

B. Lithiated Samples. Figures 1 and 2 show the XRD patterns of two selected compounds: $CuInSnS_4$ ($\alpha = 0.5$) and $Cu_{0.73}In_{1.82}Sn_{0.45}S_4$ ($\alpha = 0.23$), after different treatments with *n*-butyllithium. For both series of compounds, two sets of reflections can be seen. The first corresponds to the pristine phase. The reflections of the second, which increase in relative intensity with the amount of lithium, can be indexed according to the cubic system.

For the compound $CuInSnS_4$ (Figure 1), this lithiated phase presents a poor crystallinity. Its unit cell parameter is $a = 10.74$ Å. The spinel phase is still present after a great amount of inserted lithium (4.0 Li). In contrast, for the compound $Cu_{0.73}In_{1.82}Sn_{0.45}S_4$ (Figure 2), the narrow reflections of the new phase indicate a good crystallinity, and the spinel phase is almost totally replaced after 4.2 Li. Three important points can be noticed:

(i) The (220) reflection of the new lithiated phase is not present. Since the intensity ratio (220)/(111) is especially sensitive to the scattering factor ratio of atoms in the 8a and 16d sites, it means that the scattering factor of the atoms in the 8a sites is very low, and thus that indium atoms initially located in 8a have been displaced.

(ii) The higher intensity in the XRD of the (400) and (440) reflections for the new phase, indicates that the structure is based on an octahedral cation occupancy. In fact, these reflections can be assigned as the (200) and (220) reflections of the NaCl rocksalt structure.

(9) Denis, S.; Baudrin, E.; Touboul, M.; Tarascon, J. M. *J. Electrochem. Soc.* **1997**, *144*, 4099
(10) Young, R. A.; Sakthivel, A.; Moss, T. S.; Paiva-Santos, C. O. *J. Appl. Crystallogr.* **1995**, *28*, 366.
(11) Kündig, W. *Nucl. Instrum. Methods* **1979**, *75*, 336.
(12) Garbato, L.; Geddo-Lehmann, A.; Ledda, F. *J. Crystal Growth* **1991**, *114*, 299.
(13) Gastaldi, L.; Scaramuzza, L. *Acta Crystallogr. B* **1980**, *36*, 2751.
(14) Manolikas, C.; de Ridder, R.; van Landuyt, J.; Amelinckx, S. *Phys. Stat. Sol. A* **1980**, *59*, 621.
(15) Mähl, V. D.; Pickardt, J.; Reuter, B. *Z. Anorg. Allg. Chem.* **1982**, *491*, 203.
(16) Colombet, P.; Danot, M.; Rouxel, J. *Rev. Chim. Mineral.* **1979**, *16*, 179.
(17) Ohachi, T.; Pamplin, B. R. *J. Cryst. Growth* **1977**, *42*, 747.

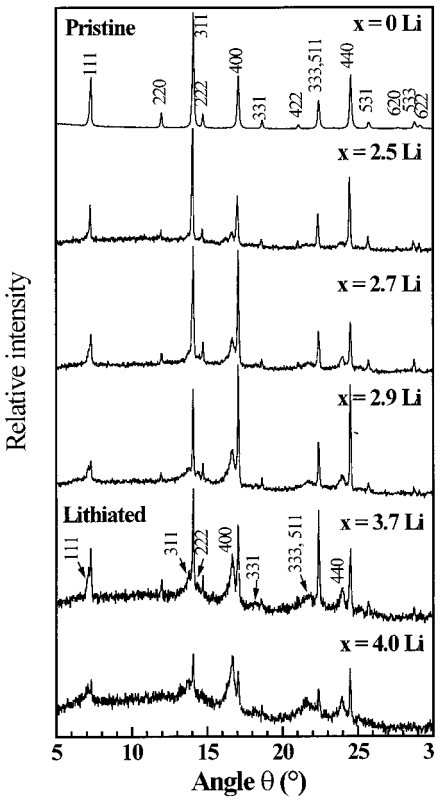

Figure 1. X-ray diffraction patterns of $CuInSnS_4$ and lithiated samples, at different lithium contents per mole of pristine compound ($\lambda_{Cu\ K\alpha} = 1.5418$ Å).

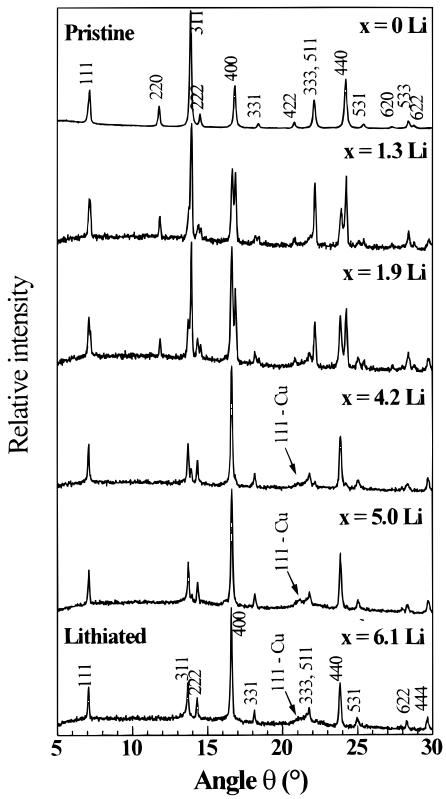

Figure 2. X-ray diffraction patterns of $Cu_{0.73}In_{1.82}Sn_{0.45}S_4$ and lithiated samples, at different lithium contents per mole of pristine compound ($\lambda_{Cu\ K\alpha} = 1.5418$ Å).

(iii) The (111) reflection of metallic copper is visible.

The first two points indicate that the new lithiated phase has a rocksalt-type structure, where no cations are present in the tetrahedral sites. Thus, In atoms present in 8a sites in the pristine compound migrate to octahedral sites during lithium insertion. This phase corresponds thus to $Li_xIn_{1.82}Sn_{0.45}S_4$, a partially ordered rocksalt structure refined in the Rietveld calculations, as exposed bellow. This behavior has been described by Thackeray et al.[2] in oxide compounds. When lithium insertion takes place in initially empty octahedral 16c sites, and when the B_2X_4 framework remains intact, A cations are displaced from 8a to 16c sites due to the electrostatic repulsion between A and Li^+ cations.

On the other hand, the (111) reflection of metallic copper indicates that copper is reduced from Cu^I to Cu^0 and extracted from the structure. This behavior has been described for the Chevrel compound $Cu_yMo_6S_8$, effect that was called "salting out".[18] It has also been observed in other copper-containing thiospinels, e.g. $CuZr_2S_4$,[3] Cu_yTiS_2,[19] and $CuCr_2S_4$.[20] The same phenomenon certainly takes place in the compound $CuInSnS_4$, but the copper reflections are difficult to identify due to the poor crystallinity of the samples.

Having in mind these results, a Rietveld refinement has been carried out for each lithiated sample of $Cu_{0.73}In_{1.82}Sn_{0.45}S_4$ with the following assumptions:

(i) The framework of the pristine phase is retained.

(ii) The occupancy of the octahedral 16d sites in the lithiated phase (12.4 In + 3.6 Sn) has not been modified by lithium insertion, as compared with the nonlithiated phase.

(iii) The occupancy of the octahedral 16c sites is 13.8 Li + 2.2 In.

(iv) No atoms are present in tetrahedral 8a sites.

Table 2 includes the results of the Rietveld refinements. The values of the reliability factors for the different samples ($R_{Bragg} < 3\%$) confirm that these assumptions are good. Thus, the structure of the lithiated phase can be considered as an ordered NaCl-type, where the particular occupation of octahedral sites results from the initial spinel structure.

We can notice that the theoretical lithium content to reach the maximum percentage of the rocksalt related phase is 1.73 Li/mol. This value is in contrast with the data exposed in Table 2, where the 100% of the rocksalt phase is obtained at only 6.1 Li/mol. This can be explained by the presence of an amorphous third phase, based on Sn^0, as Mössbauer data evidence.

In this way, Figures 3 and 4 include the ^{119}Sn Mössbauer spectra of several lithiated samples of $CuInSnS_4$ and $Cu_{0.73}In_{1.82}Sn_{0.45}S_4$. The refined hyperfine parameters are given in Tables 3 and 4. The spectra show several components. The first, at ~1.1−1.2 mm.s^{-1}, corresponds to Sn^{IV} in octahedral coordination, and its contribution decreases as the lithium content increases, indicating the reduction of Sn^{IV} during the lithium insertion process.

The second signal appears at ~3.7−3.8 mm s^{-1}, and is attributed to Sn^{II} in octahedral coordination. Its

(18) McKinnon, W. R.; Dahn, J. R. *Solid State Commun.* **1984**, *52*, 245.
(19) Jacobsen, T.; Zachau-Christiansen, B.; West, K.; Atlung, S. *Electrochim. Acta* **1989**, *34*, 1473.
(20) Imanishi, N.; Inoue, K.; Takeda, Y.; Yamamoto, O. *J. Power Sources* **1993**, *43*−*44*, 619.

Table 2. Results of the Rietveld Analysis of the X-ray Diffraction Patterns of $Cu_{0.73}In_{1.82}Sn_{0.45}S_4$ after Lithium Insertion, with $Fd\bar{3}m$ Space Group, Origin Choice 2 ($\bar{3}$m)[a]

		lithium per mol of pristine compound					
sample		0	1.3	1.9	4.2	5.0	6.1
		Pristine: Spinel Structure					
cell	a (Å)	10.595(1)	10.601(1)	10.601(1)	10.601[b]	10.601[b]	
parameters	$x_{(32e)}$	0.254(1)	0.253(1)	0.251(1)	0.251[b]	0.251[b]	
contribution	%	100	66.5(1)	51.8(1)	7.3(1)	1.7(1)	0
reliability factor	R_{Bragg}	2.92	2.15	1.79			
		Lithiated: Rocksalt-Related Structure					
cell	a (Å)		10.735(1)	10.754(1)	10.757(1)	10.758(1)	10.770(1)
parameters	$x_{(32e)}$		0.246(2)	0.246(1)	0.242(1)	0.242(1)	0.242(1)
contribution	%	0	33.5(1)	48.2(1)	92.7(1)	98.3(1)	100
reliability factor	R_{Bragg}		2.68	2.28	2.52	2.11	2.91
		Global Reliability Factors					
	R_p (%)	4.28	4.84	3.76	4.58	3.88	4.01
	R_{wp} (%)	5.54	6.09	4.70	5.77	4.85	4.96
	$R_{expected}$ (%)	5.09	5.04	4.40	5.25	3.67	4.21
	GoF	1.08	1.19	1.05	1.09	1.31	1.16

[a] Atoms have been placed in the following sites: 8a (5.8 Cu + 2.2 In), 16d (12.4 In + 3.6 Sn) and 32e (32 S) for the pristine phase and 16c (13.1 Li + 2.2 In), 16d (12.4 In + 3.6 Sn) and 32e (32 S) for the lithiated phase [b] Fixed values.

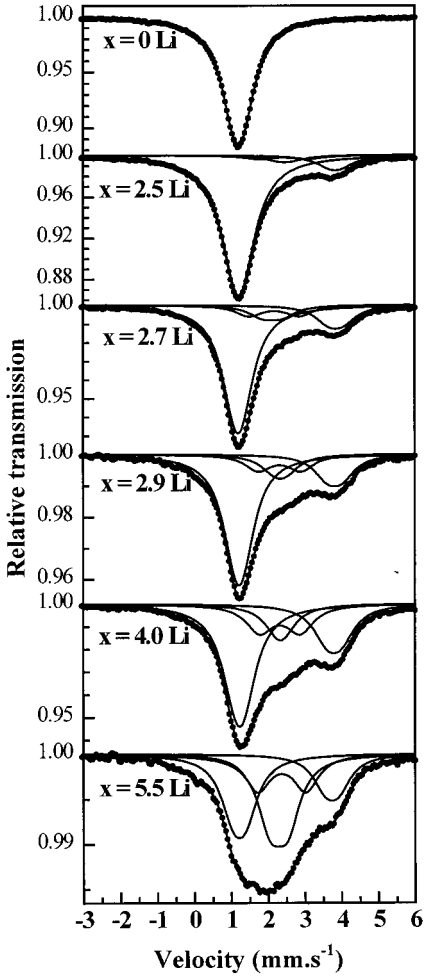

Figure 3. ^{119}Sn Mössbauer spectra of $CuInSnS_4$ and lithiated samples, at different lithium contents per mole of pristine compound..

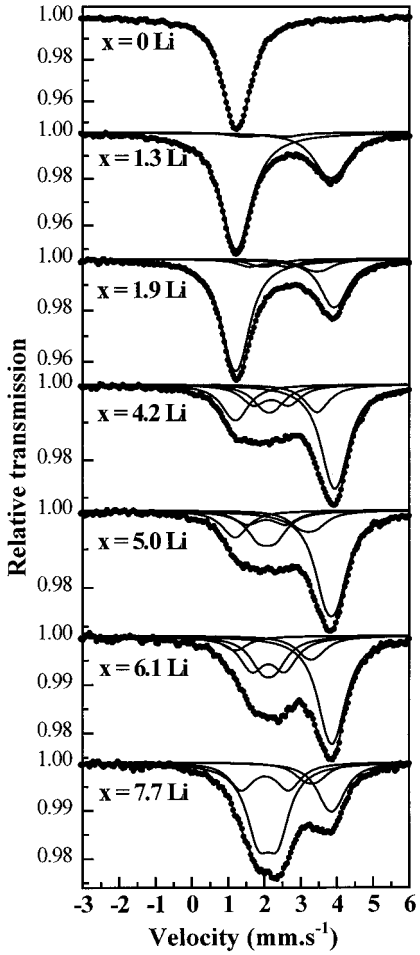

Figure 4. ^{119}Sn Mössbauer spectra of $Cu_{0.73}In_{1.82}Sn_{0.45}S_4$ and lithiated samples, at different lithium contents per mole of pristine compound.

contribution increases at the beginning of the insertion, and decreases with further lithium insertion.

The third and fourth subspectra are located in the interval 1.9−2.4 mm s^{-1}, and can be attributed to tin atoms involved in intermetallic bonds and/or clusters. The isomer shift values are similar to that observed for β-Sn[21] and also to those of Li−Sn alloys prepared electrochemically.[22] In the latter, similar values of quadrupole splitting were also observed.

Thus, Li insertion results in reduction of Sn^{IV} into Sn^{II}, and of Sn^{II} into Sn^0, with formation of an amor-

(21) Peneva, S. K.; Neykov, N. S.; Rusanov, V.; Chakarov, D. D. *J. Phys. Condens. Matter* **1994**, *6*, 2083.

(22) Chouvin, J.; Olivier-Fourcade, J.; Jumas, J. C.; Simon, B.; Godiveau, O. *Chem. Phys. Lett.* **1999**, *308*, 413.

Table 3. Hyperfine Parameters of Refined Mössbauer Spectra of $CuInSnS_4$ before and after Lithium Insertion: Isomer Shift (δ, mm s^{-1}), Quadrupole Splitting (Δ, mm s^{-1}), Full-Width at Half-Maximum (Γ, mm s^{-1}) and Relative Area (R.A., %)

		Lithium per Mole of Pristine Compound					
sample		0 Li	2.5 Li	2.7 Li	2.9 Li	4.0 Li	5.5 Li
Sn^{IV}	δ	1.12(1)	1.12(1)	1.11(1)	1.13(2)	1.14(1)	1.13(3)
	Δ	0.23(1)	0.18(1)	0.20(1)	0.20(3)	0.23(2)	0.34(3)
	R.A.	100	82.5	65.9	57.4	46.6	27.7
$Sn^0(1)$	δ		2.37(9)	2.03(3)	2.25(6)	2.2(1)	2.20(2)
	Δ		0.3(2)	0.52(5)	0.3(1)	0.1(2)	0.47(2)
	R.A.	0	4.4	9.9	11.6	13.2	34.7
$Sn^0(2)$	δ		2.34(7)	2.08(3)	2.23(6)	2.24(3)	2.29(4)
	Δ		1.4(1)	1.37(6)	1.2(1)	1.10(6)	1.31(6)
	R.A.	0	3.9	10.2	13.1	19.3	20.0
Sn^{II}	δ		3.75(2)	3.76(1)	3.72(1)	3.70(1)	3.65(2)
	Δ		0.24(4)	0.40(2)	0.40(2)	0.39(2)	0.36(3)
	R.A.	0	9.2	14.0	16.3	21.0	15.7
Γ^a		0.86(1)	0.99(1)	0.87(1)	0.86(1)	0.90(2)	0.82(2)

[a] Constrained to be equal for all components.

Table 4. Hyperfine Parameters of Refined Mössbauer Spectra of $Cu_{0.73}In_{1.82}Sn_{0.45}S_4$ before and after Lithium Insertion: Isomer Shift (δ, mm s^{-1}), Quadrupole Splitting (Δ, mm s^{-1}), Full-Width at Half-Maximum (Γ, mm s^{-1}) and Relative Area (R.A., %)

		lithium per mole of pristine compound						
sample		0 Li	1.3 Li	1.9 Li	4.2 Li	5.0 Li	6.1 Li	7.7 Li
Sn^{IV}	δ	1.14(1)	1.14(1)	1.12(1)	1.11(1)	1.11(1)	1.11[b]	
	Δ	0.29(1)	0.20(3)	0.26(1)	0.19(3)	0.16(8)	0[b]	
	R.A.	100	67.4	57.8	15.3	11.2	5.4	0
$Sn^0(1)$	δ			1.90(8)	2.05(5)	1.99(3)	2.03(9)	2.01(1)
	Δ			0.3(1)	0.30(9)	0.46(5)	0.36(18)	0.53(2)
	R.A.	0	0	4.1	12.9	18.6	18.5	49.8
$Sn^0(2)$	δ		1.94(1)	2.02(5)	2.10(4)	1.97(5)	2.03(7)	1.93(4)
	Δ		1.2(2)	1.06(6)	0.98(6)	1.06(1)	0.9(1)	1.31(5)
	R.A.	0	4.2	6.5	15.1	10.4	23.2	20.0
$Sn^{II}(1)$	δ			3.37(7)	3.37(9)	3.1(1)	3.20(7)	3.2(1)
	Δ			0.34(1)	0.1(1)	0.40(1)	0.2(1)	0.34(1)
	R.A.	0	0	6.9	11.3	10.7	9.5	9.6
$Sn^{II}(2)$	δ		3.75(1)	3.84(2)	3.86(1)	3.76(1)	3.78(1)	3.77(3)
	Δ		0.33(2)	0.24(3)	0.23(1)	0.32(2)	0.23(2)	0.23(6)
	R.A.	0	28.4	24.7	45.4	49.1	43.5	20.6
Γ^a		0.80(1)	0.95(2)	0.81(1)	0.81(1)	0.81(1)	0.83(2)	0.80(2)

[a] Constrained to be equal for all components. [b] Fixed values.

phous phase containing Sn^0. This sequence is similar to that observed in tin oxides used as electrode materials, where the tin-containing matrix plays an important role in the formation of tin alloys.[23] But in our case, the presence of a second Sn^{II} contribution visible in the spectra of $Cu_{0.73}In_{1.82}Sn_{0.45}S_4$ indicates that tin atoms in this amorphous phase are still in interaction with sulfur atoms present in the matrix. The formation of this lithium-containing amorphous phase is the reason the amount of lithium inserted in the material is greater than the amount of lithium present only in the rocksalt related phase.

There is a good correlation between the amount of spinel phase obtained by the Rietveld refinement (Table 2) and the Sn^{IV} contribution calculated from Mössbauer spectra (Table 4). This allows us to attribute Sn^{IV} to the pristine phase. Taking into account all of these results, the spinel to rocksalt transition can be represented

$$(Cu^{I}_{5.8}In^{III}_{2.2})_{8a}[In^{III}_{12.4}Sn^{IV}_{3.6}]_{16d}S_{32} + 13.1Li \rightarrow \{Li^{I}_{13.1}In^{III}_{2.2}\}_{16c}[In^{III}_{12.4}Sn^{II}_{3.6}]_{16d}S_{32} + 5.8Cu^0$$

where 13.1 is the number of lithium atoms for electroneutrality of the material.

The present results have been analyzed on the assumption that Li atoms are incorporated in octahedral 16c sites. But the occupancy of tetrahedral sites cannot be excluded a priori. To help the localization of Li atoms in the structure, some neutron experiments have been carried out. We have studied the pristine compound and one lithiated sample: 2.0 Li/mol. Figure 5 shows the experimental and refined neutron diffraction patterns. Refined parameters are included in Table 5. The best fit is obtained when no atoms are located in tetrahedral sites, thus confirming the above exposed assumptions concerning the structure of the lithiated phase. The refined occupation factor of lithium in the octahedral 16c sites was 10.0(4), which is not far from the theoretical value 13.1 for electroneutrality. An additional refinement was carried out fixing the lithium occupation factor to 13.1. The good values of the reliability factors (R_{Bragg} = 2.85 for the spinel phase and 4.43 for the rocksalt related phase, GoF = 1.58) also agree with the hypothesis. Anyway, only the fitting including the refined lithium occupancy is presented here.

C. Behavior of the Whole Family $Cu_{0.5+\alpha}In_{2.5-3\alpha}Sn_{2\alpha}S_4$ ($0 < \alpha < 0.5$). Other samples of this series were also studied: $Cu_{0.5}In_{2.5}S_4$, $Cu_{0.6}In_{2.2}Sn_{0.2}S_4$, $Cu_{0.65}In_{2.05}Sn_{0.3}S_4$, and $Cu_{0.75}In_{1.75}Sn_{0.5}S_4$ (α = 0, 0.1, 0.15, and 0.25 respectively). For these samples, a good crystallinity of the rocksalt-related lithiated phases was observed on

(23) Courtney, I. A.; Dahn, J. R. *J. Electrochem. Soc.* **1997**, *144*, 2045; 2943.

Table 5. Results of the Rietveld Analysis of the Neutron Diffraction Patterns of $Cu_{0.73}In_{1.82}Sn_{0.45}S_4$ before and after Lithium Insertion, with $Fd\bar{3}m$ Space Group, Origin Choice 2 ($\bar{3}m$)[a]

sample phase		pristine spinel $Cu_{5.8}In_{14.5}Sn_{3.6}S_{32}$	lithiated (2.0 Li per mol)	
			spinel $Cu_{5.8}In_{14.5}Sn_{3.6}S_{32}$	rocksalt-related $Li_{10.0}In_{14.5}Sn_{3.6}S_{32}$[b]
cell parameters	a (Å)	10.612(1)	10.615(1)	10.763(1)
	$x_{(32e)}$	0.255(1)	0.254(1)	0.250(1)
relative contribution (%)		100	41.5(5)	58.5(5)
reliability factors	R_{Bragg} (%)	3.68	3.15	3.65
	R_p (%)	1.92	2.82	
	R_{wp} (%)	2.51	3.59	
	$R_{expected}$ (%)	2.62	2.34	
	GoF	0.94	1.48	

[a] Atoms have been placed in the following sites: 8a (5.8 Cu + 2.2 In), 16d (12.4 In + 3.6 Sn) and 32e (32 S) for the pristine phase and 16c (10.0[b] Li + 2.2 In), 16d (12.4 In + 3.6 Sn) and 32e (32 S) for the lithiated phase. [b] Refined lithium amount.

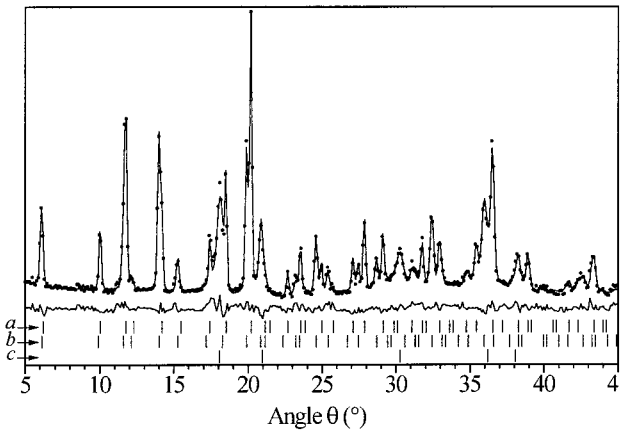

Figure 5. Experimental and refined neutron diffraction patterns of $Cu_{0.73}In_{1.82}Sn_{0.45}S_4$ after 2.0 mol of lithium inserted per mole of compound (treatment with *n*-BuLi): a → spinel phase, b → rocksalt-related phase, c → metallic copper (λ = 1.285 Å).

the XRD patterns, like the sample $Cu_{0.73}In_{1.82}Sn_{0.45}S_4$, and in contrast to $CuInSnS_4$, where the new phase presents a poor crystallinity. This behavior can be explained considering the general spinel-rocksalt transformation represented as

$$(Cu^{I}_{4+8\alpha}In^{III}_{4-8\alpha})_{8a}[In^{III}_{16-16\alpha}Sn^{IV}_{16\alpha}]_{16d}S_{32} \rightarrow \{Li^{I}_{12+8\alpha}In^{III}_{4-8\alpha}\}_{16c}[In^{III}_{16-16\alpha}Sn^{II}_{16\alpha}]_{16d}S_{32}$$

The electroneutrality is respected in the rocksalt phase if $(12 + 8\alpha) + 3(4 - 8\alpha) + 3(16 - 16\alpha) + 2(16\alpha) = 2(32)$, thus if $\alpha = 0.25$. If $\alpha > 0.25$, and in order to reduce Sn^{IV} into Sn^{II}, the necessary amount of inserted lithium is higher than the available empty sites in 16c, resulting in an important amorphization, as in $CuInSnS_4$ ($\alpha = 0.5$). On the contrary, if $\alpha < 0.25$, the electroneutrality can be respected providing that some of the 16c octahedral sites are still vacant. This explains the difference of behavior observed before.

D. Electrochemical Behavior. Electrochemical lithium insertion was carried out using the samples $CuInSnS_4$ and $Cu_{0.73}In_{1.82}Sn_{0.45}S_4$ as active electrode materials. The first cycle of discharge/charge of each compound is represented in Figure 6a, and the derivative $-dx/dV$ is represented in Figure 6b.

For the compound $Cu_{0.73}In_{1.82}Sn_{0.45}S_4$, we can observe a small plateau at 1.6 V, that corresponds to the spinel to rocksalt transformation. It can be seen in Figure 6b that this reduction step can be solved in two processes,

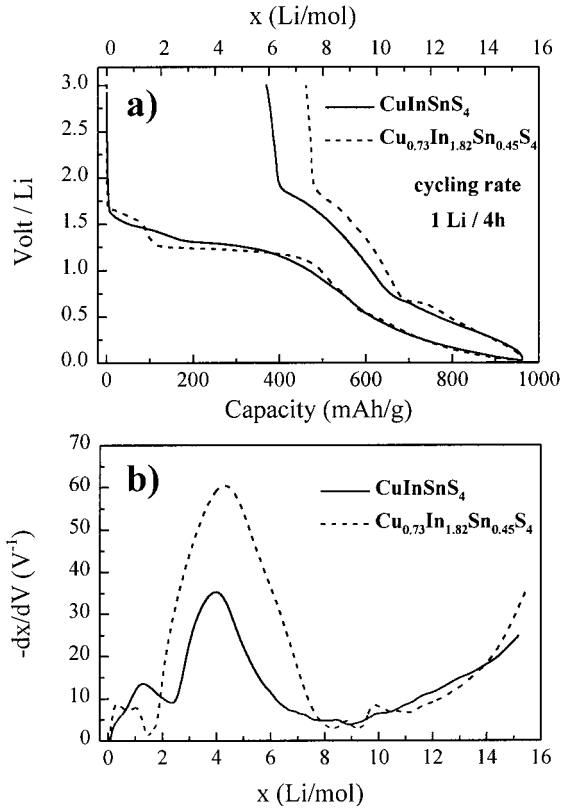

Figure 6. (a) First cycle of discharge/charge of both compounds $CuInSnS_4$ and $Cu_{0.73}In_{1.82}Sn_{0.45}S_4$ and (b) derivative $-dx/dV$.

which take place simultaneously and correspond to the extraction of metallic copper out of the structure and to the reduction of Sn^{IV} into Sn^{II}:

$$Cu^{I}_{0.73}In_{1.82}Sn^{IV}_{0.45}S_4 + 0.73\ Li \rightarrow Li_{0.73}In_{1.82}Sn^{IV}_{0.45}S_4 + 0.73\ Cu^0 \quad (45\ mAh/g)$$

$$Li_{0.73}In_{1.82}Sn^{IV}_{0.45}S_4 + 0.9\ Li \rightarrow Li_{1.63}In_{1.82}Sn^{II}_{0.45}S_4 \quad (55\ mAh/g)$$

Global:

$$Cu^{I}_{0.73}In_{1.82}Sn^{IV}_{0.45}S_4 + 1.63\ Li \rightarrow Li_{1.63}In_{1.82}Sn^{II}_{0.45}S_4 + 0.73\ Cu^0 \quad (100\ mAh/g)$$

From a quantitative point of view, the end of the first plateau of $Cu_{0.73}In_{1.82}Sn_{0.45}S_4$ is observed at $x = 1.50$ Li/mol in Figure 6b, which is in good correlation with

the theoretical value, since the amount of lithium in the rocksalt-related phase has to be $x = 1.63$ Li/mol to respect the electroneutrality, as seen before.

This reduction step is not as well defined for the compound $CuInSnS_4$ since the theoretical amount of 3 Li/mol to reduce Cu^I into Cu^0 and Sn^{IV} into Sn^{II} cannot be accommodated in the host matrix, and a simultaneously amorphization process takes place.

A second plateau is observed at 1.2 V for both compounds, which corresponds to the total reduction of the cations leading to the formation of the amorphous phase and the destruction of the rocksalt-related phase. This plateau is better defined for $Cu_{0.73}In_{1.82}Sn_{0.45}S_4$ than for $CuInSnS_4$, because in $CuInSnS_4$ the amorphization takes place earlier during the lithium insertion.

The theoretical end of the second plateau corresponds to the total reduction of the cations after 8.0 Li/mol inserted. Thus, the value observed for $Cu_{0.73}In_{1.82}Sn_{0.45}S_4$ at 8.2 Li/mol is in good correlation with the predicted value. For the compound $CuInSnS_4$, the end of the second plateau is also observed at ~8 Li/mol. The corresponding capacities are 490 and 504 mAh/g respectively for $Cu_{0.73}In_{1.82}Sn_{0.45}S_4$ and $CuInSnS_4$, which are in good agreement with the capacity values observed in the experimental discharge curves in Figure 6. These results confirm the proposed mechanism, based on the results of the chemical lithiation of the samples.

Moreover, the total discharge up to 0 V gives capacities close to 1000 mAh/g. If we model the low potential insertion process in a very simplistic way with the formation of Li−Sn and Li−In alloys, the formation of the lithium-rich phase $Li_{22}Sn_5$ corresponds to capacities of 121 and 277 mAh/g for $Cu_{0.73}In_{1.82}Sn_{0.45}S_4$ and $CuInSnS_4$ respectively, and the formation of the lithium-rich phase $Li_{13}In_3$ corresponds to capacities of 484 and 273 mAh/g respectively, to give 605 and 550 mAh/g for this alloying process, and 1095 and 1050 mAh/g at the end of the discharge.

These values agree with the values observed in Figure 6, and clearly show that both In and Sn are involved in the alloying process. Moreover, the reversible capacity values, close to 600 mAh/g (see Figures 6 and 7) confirm this hypothesis.

In conclusion, the study of the discharge curves confirms the proposed lithium insertion mechanism.

The cycling behavior of both compounds is represented in Figure 7. They show a great capacity loss of ~40% after the first cycle (from 1000 to 600 mAh/g of active compound), which is due to the irreversible formation of the amorphous phase, as exposed above. Then, their capacity decreases slowly to reach the value of 400 mAh/g after 20 cycles, that corresponds to a capacity loss of 33% compared to 600 mAh/g of the first-charge capacity.

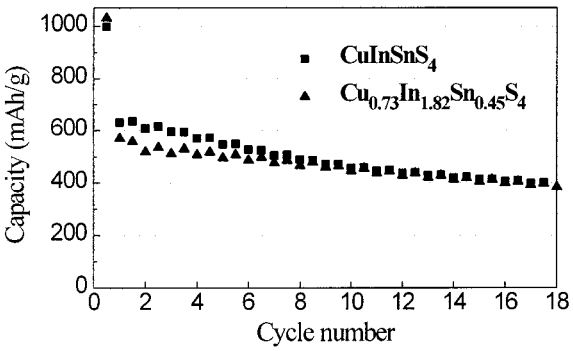

Figure 7. Capacity loss of both compounds $CuInSnS_4$ and $Cu_{0.73}In_{1.82}Sn_{0.45}S_4$ (cycling rate 1 Li/2 h, range 0−2.5 V).

Conclusion

The study of chemical lithium insertion in the compounds $Cu_{0.5+\alpha}In_{2.5-3\alpha}Sn_{2\alpha}S_4$ ($0 \le \alpha \le 0.5$) allows us to draw the following conclusions:

(i) Lithium insertion induces a multiphase reaction.

(ii) In the lithium inserted phase, In atoms migrate from tetrahedral 8a sites to octahedral 16c sites, which results in a spinel to rocksalt transformation, while Cu^I is extracted from the structure as Cu^0.

(iii) For values of α lower than 0.25, the rocksalt-related phase has a good crystallinity.

(iv) Mössbauer and XRD data allow us to attribute Sn^{IV} exclusively to the pristine phase and Sn^{II} to the lithiated rocksalt phase.

(v) Mössbauer spectra also show the presence of metallic tin in an amorphous phase (not detected by XRD and neutron diffraction).

(vi) The good capacity and the low reduction/oxidation potentials of these materials make them possible candidates as negative electrodes for lithium ion batteries.

Acknowledgment. The authors are grateful to Institute Laue-Langevin for the recording of neutron diffraction patterns, especially to Dr. Javier Campo. C.P.V. is indebted to the European Community, Training and Mobility of Researchers Program, contract number ERBFMBICT 96.0768 and 98.3020.

CM991190J